analytical chemistry

pubs.acs.org/ac Article

Subcellular Interactomes Revealed by Merging APEX with Cross-Linking Mass Spectrometry

Mengze Sun,[1] Feng Yuan,[1] Yuliang Tang, Peng Zou,* and Xiaoguang Lei*

Cite This: *Anal. Chem.* 2022, 94, 14878−14888 Read Online

ACCESS | Metrics & More | Article Recommendations | Supporting Information

ABSTRACT: Subcellular protein−protein interactions (PPIs) are essential to understanding the mechanism of diverse cellular signaling events and the pathogenesis of diseases. Herein, we report an integrated APEX proximity labeling and chemical cross-linking coupled with mass spectrometry (CXMS) platform named APEX-CXMS for spatially resolved subcellular interactome profiling in a high-throughput manner. APEX proximity labeling rapidly captures subcellular proteomes, and the highly reactive chemical cross-linkers can capture weak and dynamic interactions globally without extra genetic manipulation. APEX-CXMS was first applied to mitochondria and identified 653 pairs of interprotein cross-links. Six pairs of new interactions were selected and verified by coimmunoprecipitation, the mammalian two-hybrid system, and surface plasmon resonance method. Besides, our approach was further applied to the nucleus, capturing 336 pairs of interprotein cross-links with approximately 94% nuclear specificity. APEX-CXMS thus provides a simple, fast, and general alternative to map diverse subcellular PPIs.

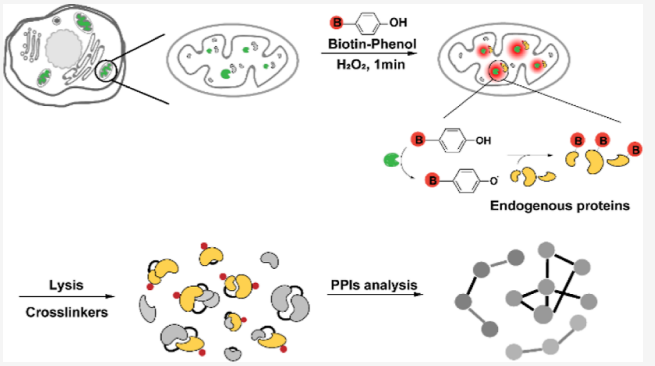

INTRODUCTION

Protein−protein interactions (PPIs) regulate many biological processes, such as cell growth and development, metabolism, and signal transduction.[1] Several techniques have been developed to study binary protein−protein interactions, including the yeast two-hybrid (Y2H) system,[2] fluorescence resonance energy transfer (FRET),[3] and protein-fragment complementation assay (PCA).[4] Affinity purification mass spectrometry (AP-MS)[5] and co-immunoprecipitation (Co-IP)[6] prefer to detect interactions among protein complexes. Surface plasmon resonance (SPR) and isothermal titration calorimetry (ITC)[7] are especially suitable for detecting interactions between purified proteins. However, advances in this area have been impeded, in part, by the lack of techniques for proteomewide profiling of transient and weak interactions at the subcellular level. Protein functions are closely related to the subcellular distribution, owing to different downstream signal pathways they mediate and different physiological environments provided by separate compartments such as antioxidants, ROS levels, and corresponding interaction factors.[8] Furthermore, dysregulated PPIs have been implicated in multiple diseases such as cancer, metabolic diseases, and neurodegenerative diseases.[9] Given the importance of mapping PPIs with high spatial and temporal resolution, chemical cross-linking methods have been combined with organelle purification pipelines to achieve subcellular PPI profiling.[10−13] However, the methods often suffer from low spatial resolution due to contamination of other subcellular compartments and are only applicable to a limited number of purifiable organelles.

Two mass spectrometry (MS)-based methods, including proximity labeling (e.g., APEX[14,15]/APEX2[16] and BioID[17,18]/TurboID[19]) and chemical cross-linking coupled with MS (CXMS), have been established to study PPIs in recent years.[20−26] Enzyme-mediated proximity labeling strategies express ascorbate peroxidase or biotin ligase in targeted areas and achieve labeling via the generation of highly reactive chemical species.[14] APEX, a monomeric peroxidase variant derived from dimeric plant ascorbate peroxidase, is developed for proximity labeling, especially spatially resolved proteomic profiling.[15] To improve the catalytic efficiency of APEX, the engineered peroxidase APEX2 is further developed by yeast-display evolution.[16] The process of APEX2-mediated proximity labeling is to express the protein of interest fused with the APEX2 enzyme, preincubate the cells with biotin-phenol, and then treat them with H_2O_2 for 1 min to generate short-lived free radicals around the peroxidase. Therefore, the labeling provides a snapshot of the local environment around the

Received: May 16, 2022
Accepted: October 10, 2022
Published: October 20, 2022

APEX2 fusion protein in the range of 10−20 nm, capturing the nearby proteins with a fast reaction kinetics and in a high-throughput manner. New chemical probes have been designed to label peptides with more vigorous MS intensity and higher specificity in the topological mapping of the targeted subcellular proteome.[27−31] While it is hard to distinguish direct interactions from indirect interactions, it mainly provides interaction networks of bait proteins instead of a systemic view of subcellular PPIs.[32] CXMS captures interacting proteins within the range of cross-linker spacer arm by forming covalent bonds, which may discover dynamic interactions.[33] It also represents a high-throughput method for globally profiling interactions and simultaneously determines the identity and connectivity of local PPIs without cell engineering. However, CXMS capturing protein interactions at the proteome level can only observe interactions among high-abundance proteins.[26] In contrast, interactions among low-abundance proteins in specific organelles remain challenging to study.

Herein, we established a platform named APEX-CXMS, which enabled us to uncover the PPIs of the target region in a high-throughput manner. We first applied this technique in mitochondria and identified 653 pairs of interprotein cross-links, including 47% reported PPIs and 53% new cross-links. Six pairs of new interactions were subsequently verified using Co-IP, mammalian two-hybrid (M2H), and SPR methods. Besides, the network comprised 37% mitochondrial cross-links. We compared its spatial specificity with CXMS in whole-cell lysates (WCLs) and in isolated mitochondria. The results showed that APEX-CXMS could enrich mitochondrial protein interactions and capture weak interactions. Additionally, we applied this method to the nucleus and observed 336 pairs of interprotein cross-links with 94% nuclear specificity, which further demonstrated the feasibility and effectiveness of APEX-CXMS in revealing subcellular PPI networks.

EXPERIMENTAL SECTION

Materials and Reagents. Tris(2-carboxyethyl) phosphine (TCEP) and 2-iodoacetamide (IAA) were purchased from Pierce Biotechnology (Thermo Scientific). HEPES, NaCl, urea, $CaCl_2$, methylamine, and DMSO were purchased from Sigma. Acetonitrile (ACN), formic acid (FA), acetone, and NH_4HCO_3 were purchased from J. T. Baker. Mass-spectrometry-grade trypsin was purchased from Promega.

Cell culture. Generation of cells stably expressing the mito-APEX2 construct was done following the method reported by Han et al.[34] Construction of APEX2-3×NLS plasmids was done following the method reported by Li et al.[35] HEK293T cells, mito-APEX2 HEK293T, and 3xNLS-APEX2 HEK293T cells were cultured in Dulbecco's modified Eagle's medium (DMEM, Gibco) supplemented with 10% (v/v) fetal bovine serum (FBS, Gibco) and 1% (v/v) penicillin/streptomycin (Gibco). The cell lines were maintained at 37 °C in 5% CO_2. APEX2 expression and biotin signal were detected by mouse-*anti*-V5 (1:1000 dilution) and SA-647 (1:2000 dilution) antibodies, respectively. For details of western blot analysis and immunofluorescence imaging, please refer to the Supporting Information.

APEX-CXMS Experiment. The HEK293T mito-APEX2 cells and APEX2-3×NLS cells were cultured in a 10 cm dish to 80−90% confluence. The cells were incubated with 500 μM biotin-phenol (BP) for 30 min at 37 °C (BP was dissolved in DMSO as 1000× solution and diluted in 37 °C DMEM with FBS). APEX labeling was initiated by treatment with 1 mM H_2O_2 for 1 min. After incubation, the cells were washed two times with quencher solution (10 mM sodium azide, 10 mM sodium ascorbate, and 5 mM Trolox). After labeling, the cells were washed with ice-cold 1×PBS and treated with an ice-cold NP-40 buffer [50 mM Tris−HCl, 150 mM NaCl, and 1% (v/v) NP-40, pH 7.4] containing freshly added protease and phosphatase inhibitor cocktails (Roche) for 15 min at 4 °C. Two milligrams of protein input (1 mg/mL) was cross-linked with disuccinimidyl suberate (DSS, synthesized by our group) at room temperature for 30 min; the reaction was quenched with 20 mM NH_4HCO_3.

MS Analysis. The liquid chromatography−tandem mass spectrometry (LC−MS/MS) analysis was performed on the Easy-nLC 1000 II HPLC system (Thermo Fisher Scientific) coupled with the Q-Exactive mass spectrometer (Thermo Fisher Scientific). Peptides were loaded on a precolumn and further separated on an analytical column with a linear reverse-phase gradient from 100% buffer A (0.1% formic acid in H_2O) to 28% buffer B (0.1% formic acid in acetonitrile) in 60 min at a flow rate of 200 nL/min. The top 10 most intense precursor ions from the full scan (300−2000; resolution: 70,000 for MS1) were isolated for a high-energy collision dissociation MS2 system (resolution: 17,500; normalized collision energy: 27%) with a dynamic exclusion time of 30 s. Precursors with unassigned charge states or charge states of 1+, 2+, and >6+ were excluded. Cross-linked proteins were identified by pLink software.

MitoKit-CXMS. Mitochondria were isolated from cultured cells in isotonic mitochondrial isolation buffer (250 mM sucrose, 1 mM EDTA, 10 mM HEPES, pH 7.5, and 1 mM phenylmethylsulfonyl fluoride) on ice. The suspension was centrifuged twice at 800×*g* for 10 min at 4 °C to remove nuclei and cell debris. Mitochondria were pelleted by centrifugation at 10000×*g* for 10 min at 4 °C. 2 mg protein input was used in the subsequent cross-linking experiment, and cross-linking conditions were the same as those used in the APEX-CXMS experiment.

WCL-CXMS. Total cell lysates were prepared by scraping cells from Petri dishes in ice-cold NP-40 buffer. 2 mg WCLs were treated with DSS at room temperature for 30 min; the reaction was quenched with 20 mM NH_4HCO_3. Protein precipitation was carried out by using an ice-cold solution of chloroform and methanol mixed in a 4:1 ratio with the cell lysates overnight to remove extra small moleculars. Proteins were re-dissolved using Tris buffer (8 M urea in 100 mM Tris−HCl, pH 8.0) for subsequent in-solution digestion and LC−MS/MS detection.

Coimmunoprecipitation. HEK293T cells were transfected with plasmids containing selected targeting proteins fused with Flag-tag and Myc-tag (plasmids: Flag-CH10/Myc-HSPE1-MOB4, Flag-GRP75/Myc-OTUB2, Flag-GRP78/ODP2, Flag-HS71B/Myc-HS71L, Flag-HS12/Myc-H1T, and Flag-HNRC2/Myc-RALYL) and grew for 48 h. After being washed with PBS, the cells were lysed with NP-40 buffer [150 mM NaCl, 50 mM Tris−HCl pH 7.4, 1% NP-40, and protease inhibitor cocktail (Roche)] and incubated with anti-Flag beads at 4 °C for 3 h. Nonspecific proteins were washed by washing buffer (50 mM Tris−HCl, 150 mM NaCl, pH 7.4) three times, and Flag-tagged proteins and their interactors were eluted by competing with FLAG peptide in elution buffer (50 mM Tris−HCl, 150 mM NaCl, 100 μg Flag-peptide/ml, pH 7.4) for 2 h.

The immune complex was detected by a c-Myc antibody. For immunoblotting, protein samples were resolved by SDS-

https://doi.org/10.1021/acs.analchem.2c02116
Anal. Chem. 2022, 94, 14878−14888

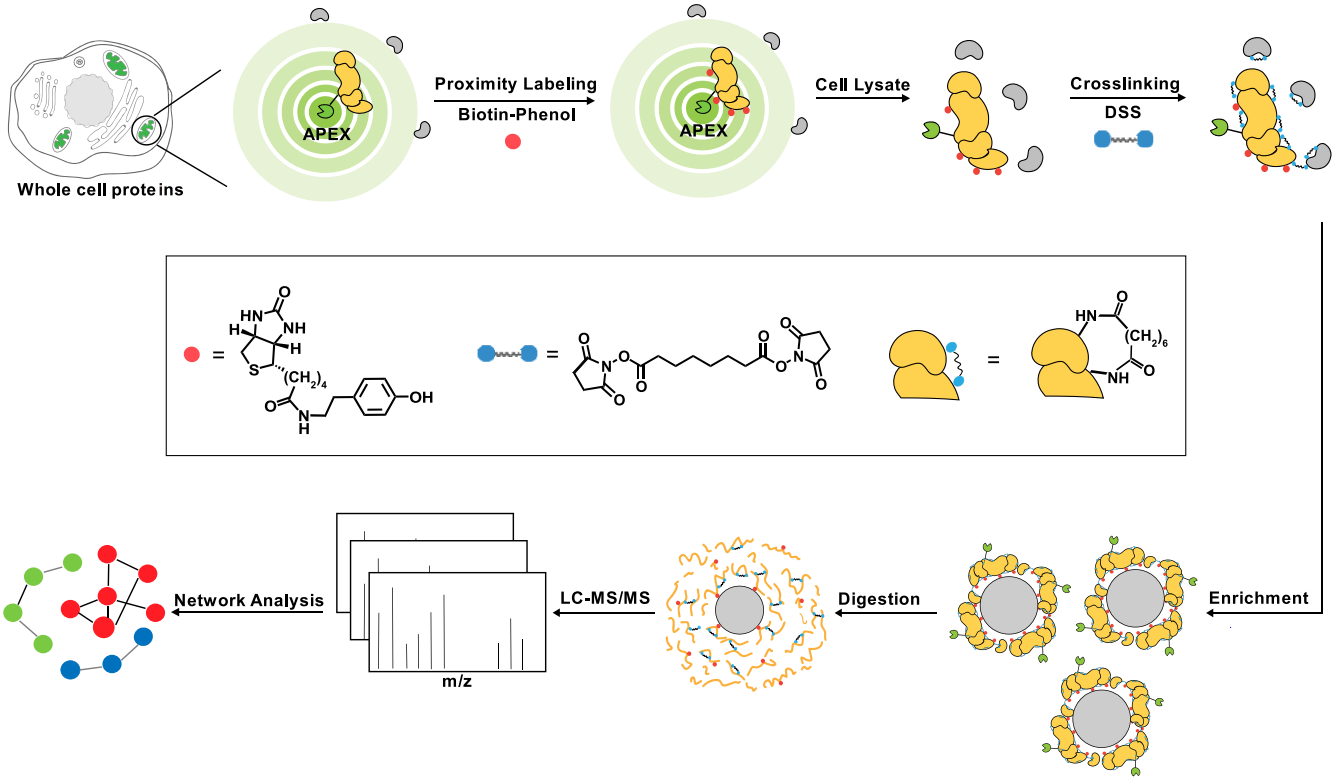

Figure 1. Workflow of APEX-CXMS for subcellular protein−protein interactions. First, the stably transfected mito-APEX2 cells were constructed, incubated with biotin-phenol, and initiated by treatment with H_2O_2. Next, a DSS cross-linker was added to the cell lysate to crosslink neighboring proteins. Biotinylated proteins labeled by the APEX2 enzyme were captured by streptavidin-agarose beads, followed by on-bead digestion. Eluted peptides were detected by LC−MS/MS and identified via pLink software.[37]

PAGE and transferred to nitrocellulose membranes. The blots were probed with the following primary antibodies: mouse monoclonal *anti*-Flag (Sigma, St. Louis, MO) or mouse monoclonal *anti*-Myc at 1:5000 (Sigma, St. Louis, MO). The secondary antibodies were goat anti-mouse IgG (Jackson ImmunoResearch, West Grove, PA) at 1:10,000 dilution.

Mammalian Two-Hybrid System. HEK293T cells were cultured in 96-well culture plates and transfected with plasmids (Supporting Information XLSX file 1) using the transfection reagent polyethyleneimine (PEI). The pACT and pBIND fusion constructs along with the pG5-Luc vector were transfected into mammalian cells in each dish in a mix of 1:1:2 ratio of pACT/pBIND/pG5-Luc in DMEM without serum. The media was replaced with fresh DMEM (10% serum) 5 h after incubation. Cells were lysed 2 to 3 days after transfection. The amount of Renilla luciferase and firefly luciferase were quantitated according to the manufacturer's instruction of a dual-luciferase reporter assay system.

SPR Detection. SPR experiments were conducted using a Biacore T200 instrument (GE Healthcare), and CM5 chips were used for protein fixation. The running buffer contained 10 mM HEPES, pH 7.5, 150 mM NaCl, 3 mM EDTA, and 0.005% v/v surfactant P20. Binding affinity and kinetics of the two interacting proteins were analyzed using Biacore T200 Evaluation software (version 2.0, GE Healthcare).

RESULTS

APEX-CXMS for Profiling Mitochondrial Protein−Protein Interactions. To profile dynamic and weak subcellular protein interactions globally, we designed the APEX-CXMS workflow, which combines *in situ* APEX labeling with covalent chemical cross-linking (Figure 1). This was initially applied to profiling mitochondrial PPIs. First, we constructed the mito-APEX2 cells which express the APEX2 enzyme in the mitochondrial matrix via fusion to a 24-amino acid-targeting peptide.[14] Next, the DSS cross-linker was added to the cell lysate. The reactive group in DSS, *N*-hydroxysuccinimide (NHS) esters, preferentially reacts with primary amines and cross-links lysine residues or protein *N*-terminus within the distance of the DSS spacer arm by forming stable amide bonds,[36] providing accurate and systematic protein interaction interface information.

First, we evaluated the efficiency and specificity of APEX labeling, and the results showed that the APEX2 enzyme was successfully expressed in the mitochondrial matrix with a strong labeling signal (Figure 2A, left); the immunofluorescence experiment indicated that APEX labeling had high spatial specificity (Figure 2A, right). Then, CXMS experiments were performed, and APEX-CXMS can provide more comprehensive information on mitochondrial cross-links between two residues of proteins with different sequences (referred to as "PPI-links" for simplicity) than conventional methods. 653 pairs of cross-linked proteins were identified, of which 47% were reported in STRING, DIP, BioGRID, and IntAct databases (Figure 2B). Cross-links captured by APEX-CXMS included many protein interactions that were previously detected by traditional methods, such as interactions between mitochondrial respiratory chain complexes and metabolic enzymes in mitochondria (Supporting Information XLSX file 1), proving the feasibility and reliability of our approach for investigating protein−protein interactions. 346 pairs of unique cross-links (accounting for 53%) were

https://doi.org/10.1021/acs.analchem.2c02116
Anal. Chem. 2022, 94, 14878−14888

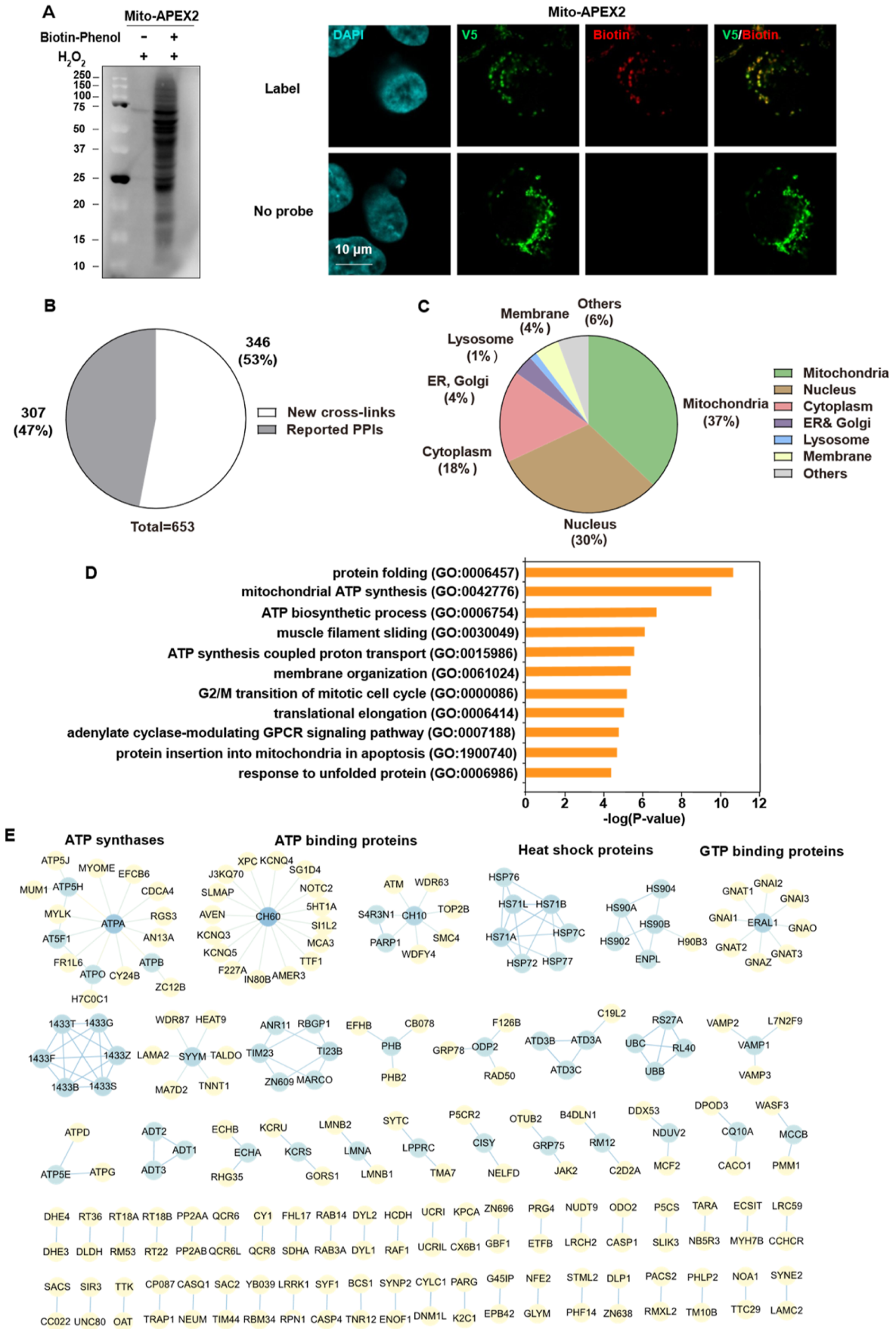

Figure 2. Demonstrating APEX-CXMS as an effective combinatorial technique to study mitochondrial PPIs. (A) Labeling efficiency and spatial specificity of the APEX2 enzyme by the western blot analysis and immunofluorescence experiment. Anti-V5 (green) was used to visualize APEX2

https://doi.org/10.1021/acs.analchem.2c02116
Anal. Chem. 2022, 94, 14878−14888

Figure 2. continued

expression; DAPI (blue) was used to stain DNA; SA-647 (red) was to verify the biotinylation signal for detecting the labeling efficiency. (Scale bars: 10 μm.) (B) Reported PPIs and new cross-links identified in three APEX-CXMS replicates. (C) Spatial specificity of cross-linked proteins. (D) Gene ontology analysis of identified proteins by APEX-CXMS. (E) Mitochondrial PPI network identified by APEX-CXMS. Darker color indicates more annotation of proteins in Uniprot; a node tends to be blue instead of yellow when it has more functional and structural annotation information. Similarly, a darker edge means that the interactions between proteins at both ends of the connection have been studied more comprehensively in the literature.

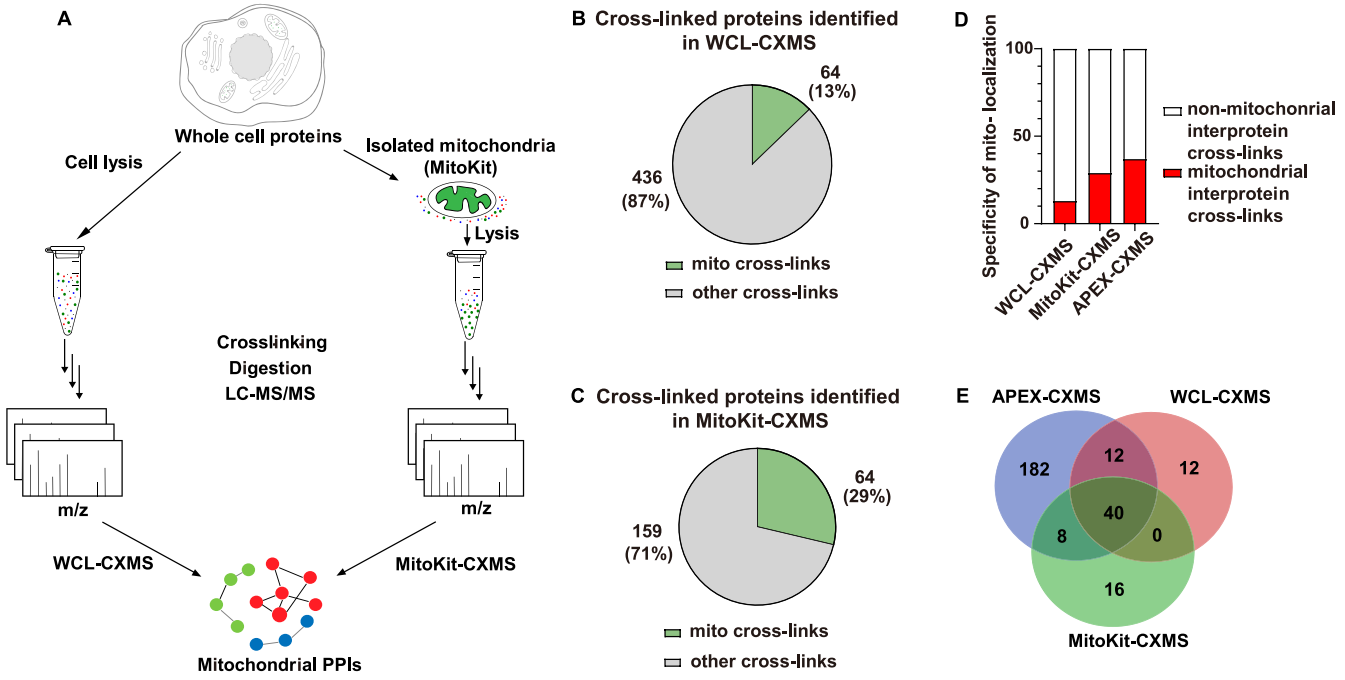

Figure 3. Evaluation of the spatial specificity of APEX-CXMS. (A) Procedure of the CXMS assay in WCLs (WCL-CXMS) and isolated mitochondria separated by MitoKit (MitoKit-CXMS). (B) Spatial specificity of cross-linked proteins identified in WCL-CXMS. (C) Spatial specificity of cross-linked proteins identified in MitoKit-CXMS. (D) Comparison of the spatial specificity of APEX-CXMS with the results of WCL-CXMS and MitoKit-CXMS. (E) Overlap of mitochondrial cross-links identified by the three methods.

identified in this study. We annotated the subcellular localization of cross-linked proteins, 37% of the identified cross-links have mitochondrial localization (Figure 2C), including cross-links of dual mitochondrial proteins and cross-links between the mitochondrial protein and other localization proteins (Figure S1A,B); most of the contaminated proteins came from the nucleus and cytoplasm (Figure 2C). One explanation for contaminated proteins is that cross-links were pulled down by agarose beads nonspecifically due to high abundance of nuclear proteins. Another explanation is that these mitochondrial proteins that are cross-linked with non-mitochondrial proteins have multiple assigned subcellular locations (such as the nucleus, cytoplasm, endoplasmic reticulum lumen, etc.). Once the cross-linker is added to mito-APEX2 cells, mitochondrial proteins in the process of dynamic transport and communication between different organelles will be covalently cross-linked with the surrounding proteins. We also analyzed the components in washing solution, and a small number of mitochondrial interactions were indeed detected (such as HSPA1A/HSPA1L, HSPA6/HSPA1L, and HSPA8/HSPA1L) (Supporting Information XLSX file 1).

We further analyzed the subcellular localization of identified proteins in both reported cross-links and new cross-links. Cross-links with mitochondrial localization accounted for 25% of the reported cross-links (Figure S1A), while this proportion was 48% in new cross-links (Figure S1B). We proposed several reasons for the high abundance of mitochondrial proteins in the new cross-links. First, APEX labeling identifies mitochondrial proteins in physiological conditions more accurately[14] compared to traditional methods, which isolate mitochondria by density gradient centrifugation. Second, dynamic and weak interactions may be lost using traditional methods due to cell lysis and complicated elution steps. Moreover, nonspecific cross-links might also contribute, and this is further clarified in the discussion. Subcellular localization and function of proteins in new cross-links were analyzed. Cross-links with dual mitochondrial localization (e.g., CX6B1 and KPCA, CISY, and P5CR2), and cross-links between mitochondria and other organelle-localized proteins (e.g., GRP75 and OTUB2, ATP5H and MUM1, and CH60 and AVEN) were identified (Supporting Information XLSX file 1).

Gene ontology analysis indicates that most cross-linked proteins are involved in protein folding and mitochondrial metabolic pathways (Figure 2D), mainly due to strong interactions between protein chaperones and their client proteins, and the tight association of protein subunits within metabolic enzyme complexes. Next, identified cross-links were visualized by Cytoscape software and clustered by protein function, and several interactions in mitochondrial respiratory chain complexes and metabolic enzymes were identified; the first large cluster is the ATP synthase family (Figure 2E). We

https://doi.org/10.1021/acs.analchem.2c02116
Anal. Chem. 2022, 94, 14878−14888

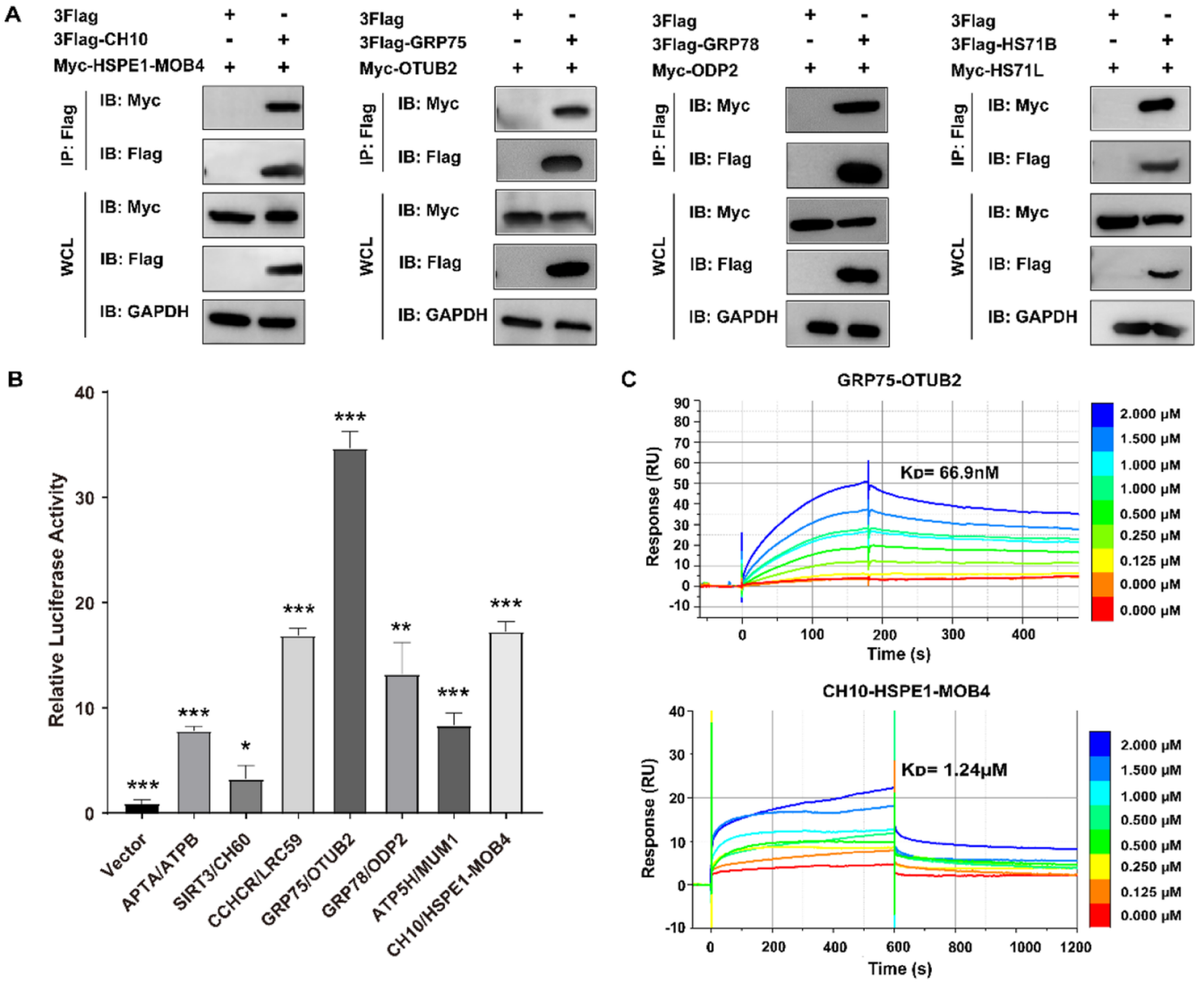

Figure 4. Three methods to validate protein interactions between new cross-links obtained by APEX-CXMS. (A) Co-IP results for validating new interactions. Immunoprecipitation was performed using *anti*-Flag conjugated beads; protein binders were probed with a c-Myc antibody. GAPDH was used as a loading control. (B) M2H results for validating new interactions. The background level of luciferase was measured using a negative control [abbreviated as a vector in the presence of GAL4 (from pBIND) and VP16 (from pACT)]. The y-axis showed relative luciferase activity as Fluc/Rluc, relative to the negative control. ATPA/ATPB and SIRT3/CH60 were positive controls. All data were the mean of at least three independent experiments. Error bars indicate standard deviation. (C) SPR results for measuring the binding affinity and kinetics of selected cross-links. The upper panel showed the response curve and dissociation equilibrium constant of GRP75/OTUB2; the lower panel showed the response curve and dissociation equilibrium constant of CH10/HSPE1-MOB4.

also identified interactions between PHB and PHB2, which are located in the mitochondrial inner membrane and closely related to physiological processes such as the inhibition of cell proliferation and induction of apoptosis.[38]

Compared with the traditional PPI detection methods, such as Co-IP which requires high-specificity antibodies, AP-MS which undergoes complicated washing steps, and FRET which requires fusion of two target proteins and has low throughput, APEX-CXMS has several advantages. First, we could detect multiple pairs of protein interactions in a high-throughput manner through one experiment. Second, interaction sites and interface of cross-linked proteins were provided. Furthermore, most identified proteins are cross-linked between mitochondrial metabolism complexes (such as enzymes in tricarboxylic acid cycle and oxidative phosphorylation), which may be caused by a limited spacer arm length of chemical cross-linkers, suggesting that different types of protein interactions will be identified by combining different cross-linkers with varying arm lengths.

Comparison of APEX-CXMS with Conventional Methods. We analyzed the spatial specificity of the APEX-CXMS technique. Cross-links with mitochondrial localization identified in our work were compared with those obtained by the CXMS assay conducted in isolated mitochondria (MitoKit-CXMS) and WCL (WCL-CXMS) (Figure 3A). Cells used for MitoKit-CXMS and WCL-CXMS experiments were not labeled by the APEX2 enzyme. We optimized the concentration of DSS in three systems to ensure that the maximum amount of cross-links can be obtained without over-cross-linking and protein precipitation. 13 and 29% cross-links which had mitochondrial localization were identified in WCL-CXMS (Figure 3B) and MitoKit-CXMS (Figure 3C), respectively. While other cross-linked proteins were from the nucleus, cytoplasm, and other organelles, such as cross-links in the

https://doi.org/10.1021/acs.analchem.2c02116
Anal. Chem. 2022, 94, 14878−14888

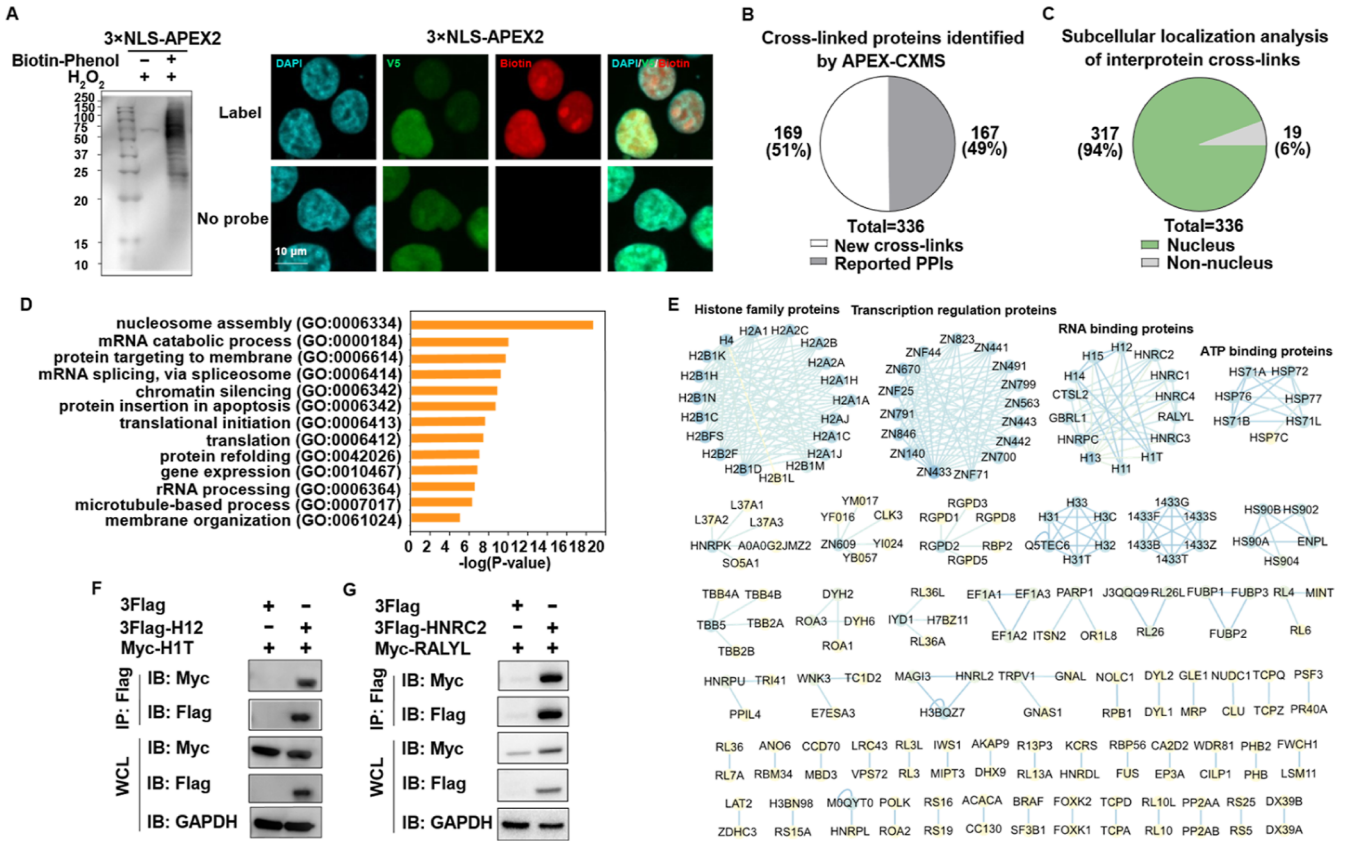

Figure 5. Application of APEX-CXMS for mapping the nuclear PPI network. (A) Labeling efficiency and spatial specificity of APEX2-NLS cells by western blot analysis and the immunofluorescence experiment. Anti-V5 (green) was used to visualize APEX2 expression; DAPI (blue) was used to stain DNA; SA-647 (red) was used to verify the biotinylation signal for detecting the labeling efficiency. (Scale bars: 10 μm.) (B) Reported PPIs and new cross-links identified in three APEX-CXMS replicates. (C) Nuclear specificity of interprotein cross-links. (D) Gene ontology analysis of identified proteins by APEX-CXMS. (E) Nuclear PPIs identified in three APEX-CXMS biological replicates; the PPIs network was visualized by Cytoscape software and identified cross-links are clustered according to protein functions. (F) Co-IP results for validating the H12/H1T interaction. (G) Co-IP results for validating the HNRC2/RALYL interaction. Immunoprecipitation was performed using *anti*-Flag conjugated beads; protein binders were probed with a c-Myc antibody. GAPDH was used as a loading control.

heterogeneous nuclear ribonucleoprotein C-like protein complex, RNA binding RALYL-like proteins, and heat shock 70 family proteins (Supporting Information XLSX files 2 and 3).

We compared the number of cross-linked proteins identified by MitoKit-CXMS with the literature[12] (Figure S2A). Although different instruments were used (see Supporting Information XLSX file 2 for details), GO analysis showed that cross-links related to mitochondrial ATP transmembrane transport and ATP synthesis were both identified by MitoKit-CXMS and by Rappsilber's method[12] (Supporting Information XLSX file 2). Unique cross-linked proteins captured in the MitoKit-CXMS study (Figure S2B) were primarily involved with protein refolding (GO: 0042026), cellular response to unfolded proteins (GO: 0006986), and positive regulation of protein insertion into the mitochondrial membrane in apoptosis (GO: 1900740), while proteins involved in depurination and nucleosome assembly (Figure S2C) were identified in their work.[12]

To evaluate the validity of cross-linking, several cross-links with mitochondrial localization were mapped to the protein structure (Figure S3A). Seven mitochondrial proteins with available high-resolution structures were used in this part, including four enzymes of primary mitochondrial metabolism (P5CS, GLYM, THIL, and OAT), mitochondrial transcription factors (TFAM), proteins related to mitochondrial protein synthesis (SYDM), and mitochondrial molecular chaperones (CH10−CH60 human mitochondrial chaperonin complex). Totally, 32 out of 37 cross-links were successfully fit into structures (Figure S3A), with 86% of cross-links falling within 35 Å (Supporting Information XLSX file 2), confirming the viability of the identified cross-links.

We compared the proportion of identified cross-links with mitochondrial localization by three different methods (APEX-CXMS, WCL-CXMS, and MitoKit-CXMS). APEX-CXMS showed the highest spatial specificity, followed by MitoKit-CXMS, and the least effective process was WCL-CXMS (Figure 3D). Compared to the cross-linking results in WCLs, APEX-CXMS integrated the APEX labeling technology and enriched mitochondrial proteins, thus increasing the number of identified mitochondrial cross-links. Additionally, APEX-CXMS is compatible with the harsh washing conditions, removing more protein contaminants than in MitoKit-CXMS. Notably, 40 pairs of mitochondrial cross-links were identified by all three methods (Figure 3E). 61% of the proteins (20 out of 33) are highly abundant in mitochondria (Supporting Information XLSX files 2 and 3). Besides, APEX-CXMS captures the majority of mitochondrial PPIs observed in the MitoKit-CXMS and WCL-CXMS experiments, 75 and 81%, respectively (Figure 3E), suggesting the sensitivity and the

https://doi.org/10.1021/acs.analchem.2c02116
Anal. Chem. 2022, 94, 14878−14888

depth of data analysis of APEX-CXMS in subcellular protein interaction detection. Unique cross-links were also observed using three methods, and the highest proportion of new cross-links were identified by APEX-CXMS. We proposed that APEX-CXMS could capture interactions during the communication process between mitochondria and other organelles, thus reducing the loss of low-abundance and dynamic interactions information compared to the other two methods.

We also compared the identified number of mitochondrial cross-linked proteins via the in vivo CXMS experiment with that by the three abovementioned methods (APEX-CXMS, WCL-CXMS, and MitoKit-CXMS), which suggested that APEX-CXMS significantly increased the identified number of mitochondrial cross-linked proteins due to the enrichment of biotinylated proteins labeled by APEX2 enzymes (Supporting Information XLSX files 1 and5), while the identified mitochondrial cross-linked proteins by other three methods showed no significant quantitative difference. Consequently, APEX-CXMS might enrich the neighboring interacting proteins, thus identifying more interprotein cross-links.

Verification of Unknown Cross-Linked Protein Interactions by the Three Methods. Six pairs of new interactions were selected for further validation according to protein function and identification frequency in multiple biological replicates (Figure S3B), including two pairs of cross-linked proteins with dual mitochondrial localization and four pairs of cross-linked proteins with one mitochondrial localization. Subsequently, other traditional methods were used to verify their interactions.

Co-IP is a classical and efficient method to study protein interactions based on the specific interaction between antibodies and antigens,[6] an appropriate Co-IP system requires highly specific antibodies to target proteins. To verify interactions of new cross-links identified by APEX-CXMS, plasmids containing selected targeting proteins fused with Flag-tag and Myc-tag were constructed and transiently transfected into HEK293T cells. Results showed that four interactions (CH10/HSPE1-MOB4, GRP75/OTUB2, GRP78/ODP2, and HS71B/HS71L) were detected using the Co-IP method (Figure 4A). The other two cross-links (CCHCR/LRC59 and ATP5H/MUM1) were not detected. Their interactions might be weak, and proteins might have been washed away in the washing steps.

To capture dynamic protein interactions and maintain post-translational modifications, such as glycosylation, phosphorylation, and acylation, the mammalian two-hybrid system was used to validate interactions of selected cross-links. Genes encoding two potentially interacting proteins were cloned into the pBIND and pACT vectors, and pBIND expresses Renilla luciferase, which is used for normalization. Increased reporter activity (Fluc/Rluc) was observed in five pairs of cross-linked proteins (Figure 4B). By comparing the relevant luciferase signals, we found that the interaction intensity of the CH10/HSPE1-MOB4 pair and GRP75/OTUB2 pair was strong, which was consistent with the results of Co-IP, followed by interactions of GRP78/ODP2 and CCHCR/LRC59. ATP5H/MUM1 interaction is relatively weak.

In addition to the abovementioned methods for detecting interactions at the cellular level, we also expressed CH10, HSPE1-MOB4, GRP75, and OTUB2 proteins in Escherichia coli (Figure S4); binding affinity of cross-linked proteins (GRP75/OTUB2 and CH10/HSPE1-MOB4) were measured by the SPR experiment. It showed that the K_D value of GRP75 and OTUB2 was 66.9 nM (Figure 4C, up), and their binding and dissociation were slow. Binding affinity of CH10 and HSPE1-MOB4 was 1.24 μM (Figure 4C, down). The results further demonstrated the potential of APEX-CXMS for capturing weak interactions.

Expanding the Application of APEX-CXMS to Other Organelles. To demonstrate the generality of APEX-CXMS, we further apply this technique to explore PPIs in the nucleus. Western blot analysis and the immunofluorescence assay showed that the APEX2 enzyme was successfully expressed for the solid-labeling signal with high spatial specificity (Figure 5A). 336 pairs of cross-linked proteins were identified in three biological replicates. 49% of them were reported using traditional methods (Figure 5B), including histone interactions (H11/H12, H33/H3C, and H4/H33) (Supporting Information XLSX file 4), RNA-binding protein interactions (HNRC1/RALYL and ROA1/RA1L2) and transcription regulation interactions (FUS/RBP56 and DDX5/DDX17) (Figure S5). Subcellular localization of cross-linked proteins was annotated (Supporting Information XLSX file 4), and 94% of the identified cross-links had nuclear localization (Figure 5C), including cross-links with dual nuclear proteins and cross-links with only one nuclear protein (Figure S1C,D). Novel cross-links between nuclear and other localized proteins were observed (e.g., nuclear and cytoplasmic cross-links ROA2/DYH6, PARP1/ITSN2, and HNRC3/GBRL1; nuclear and membrane cross-links PARP1/OR1L8 and L37A2/HNRPK; nuclear and mitochondrial protein cross-link HNRDL/KCRS; nuclear and Golgi protein cross-link DHX9/AKAP9 and so forth) (Supporting Information XLSX file 4). Most nuclear proteins that can be cross-linked with other organelles (e.g., ROA2, PARP1, and DHX9) are proteins with multiple assigned subcellular locations, implying that cross-links may be captured as a nuclear protein shuttle between the nucleus and other organelles. This result, together with previous mitochondrial cross-linking results, further supports the hypothesis that APEX-CXMS can capture protein interactions in communication of multiple organelles.

GO analysis showed that most cross-linked proteins were related to nucleosome assembly and gene expression (Figure 5D). Then, identified cross-linked proteins were visualized using Cytoscape software and clustered according to protein functions. The first large cluster was the histone family, and other clusters such as the interaction network of the zinc finger protein family, RNA binding proteins, and the heat shock protein family were also observed (Figure 5E). Subsequently, several new interactions were selected for validation by Co-IP according to the identified frequency. The H12/H1T interaction related to chromatin condensation (Figure 5F) and the HNRC2/RALYL interaction involved in RNA binding were validated (Figure 5G). Consequently, APEX-CXMS could also be extended to detect nuclear PPIs.

DISCUSSION

This work highlights that the combinatorial technique APEX-CXMS can provide more comprehensive information on mitochondrial protein interactions than conventional methods. A previous CXMS study of the isolated human mitochondria has reported 5518 pairs of cross-links, among which only 152 pairs are PPI-links.[12] The percentage of mitochondrial PPI-links (7.3%, 241 pairs) identified by APEX-CXMS is higher than that determined by the traditional CXMS assay of the intact human mitochondria (2.4%, 134 pairs).[12] There are

https://doi.org/10.1021/acs.analchem.2c02116
Anal. Chem. 2022, 94, 14878−14888

several possible explanations. First, the APEX2 enzyme labels mitochondrial proteins accurately and efficiently in physiological conditions[14] than that achieved by Rappsilber's approach,[12] and a large amount of protein loss was introduced by centrifugation during the extraction of intact organelles. Second, because of the harsh washing steps in APEX labeling, APEX-CXMS has higher spatial specificity and fewer contaminated proteins. We hypothesize that the proteins prone to interaction with other proteins are more likely to be labeled by APEX enzymes, while the protein mixture extracted from intact organelles may contain many randomly non-interacting proteins.

APEX-CXMS can also explore interorganelle interactions, such as interactions in the protein transport and organelle localization and dynamics,[39] which might be lost during organelles extraction required by other approaches. Interactions of some subcellular compartments that are difficult to separate by density gradient centrifugation can be detected, such as membraneless organelles or intermediate structures formed during communication between cells or organelles. For example, membrane protein interactions in the presynaptic membrane of nerve cells, endoplasmic reticulum−Golgi intermediate compartment (ERGIC), and interactions between mitochondria and endoplasmic reticulum are challenging to study using conventional methods. Moreover, the APEX-CXMS technique can also construct a specific protein of interest's refined interactome by fusing it with the APEX2 enzyme. Such an independent interactome of a protein in different subcellular compartments is generally challenging to be separated by density gradient centrifugation.

However, the cross-linking results may contain some false positive cross-linking products, mainly for two reasons. The first is derived from intrinsic limitations of the chemical cross-linking technique. Due to the high reactivity of the chemical cross-linkers, while stabilizing transient protein interactions, it may also contain some false positive cross-links caused by two spatially adjacent proteins. On the other hand, considering that cross-linking is performed after lysis, interacting protein pairs, which were not in the same subcellular compartment in physiological conditions, may also be mixed and lead to the undesired cross-linking products. While we cannot rule out the possibility that these are false-positive cross-links in the cell lysates with current data, it may also suggest that some bona fide interactions of interorganelle communication exist.

Several pairs of these cross-links were chosen for subsequent verification. We have validated one of these pairs by testing GRP75/OTUB2 via Co-IP, M2H, and SPR experiments. In contrast, subsequent cellular and animal experiments can be conducted to understand whether such an interaction is functionally important in physiological conditions. Although some researchers have developed in vivo cross-linking probes to directly cross-link at the cellular level and identify protein interactions closer to physiological conditions,[40−42] they also have the problems at the expense of the number of interprotein cross-links in low-abundance subcellular compartments (Figure S6). APEX-CXMS may be complementary to the in vivo cross-linking.

In summary, APEX-CXMS describes a comprehensive subcellular PPIs network on three levels: excellent sensitivity for low abundance and dynamic interactions; broad coverage for interorganelle interactions; good spatial selectivity for specific protein interaction groups in multiple compartments. By fusing the APEX2 enzyme with proteins of interest in different regions, APEX-CXMS may provide a systematic view of interorganelle interactions or any functional protein's specific interactome.

CONCLUSIONS

In this study, we combined APEX proximity labeling with the CXMS technique to profile the subcellular interactome in a high-throughput manner. We demonstrated the feasibility of APEX-CXMS for capturing protein interactions in both the mitochondria and the nucleus. We identified 653 pairs of interprotein cross-links in mito-APEX2 cells, of which mitochondrial cross-links accounted for 37%. 307 pairs of reported interactions were detected using APEX-CXMS, accounting for 47% of all identified cross-links, which indicated that APEX-CXMS is a reliable technique for studying subcellular protein interactions. Six pairs of new interactions were verified by Co-IP, SPR, and M2H methods, emphasizing the potential of this approach for discovering new interactions. Furthermore, APEX-CXMS was applied to the nucleus. 94% of the identified cross-linked proteins had nuclear localization. Two novel nuclear interactions were verified by the Co-IP assay. Overall, we demonstrated the feasibility of APEX-CXMS to capture protein interactions both in the mitochondria and the nucleus. In the future, APEX-CXMS will complement with other protein interaction detection methods and provide a new perspective for constructing a more integrated protein interaction network.

DATA AVAILABILITY

The MS raw data of APEX-CXMS analysis, CXMS assay of isolated mitochondria, and whole-cell lysis in this study were deposited at the ProteomeXchange Consortium via the iProX partner repository with the dataset identifier PXD033838. All other data are available from the corresponding authors on reasonable request. Source data are provided in this paper.

ASSOCIATED CONTENT

Supporting Information

The Supporting Information is available free of charge at https://pubs.acs.org/doi/10.1021/acs.analchem.2c02116.

Materials, protocols and data characterizations for all chemical and biological experiments (PDF)

Cross-links identified by APEX-CXMS in mitochondria, including inter-protein cross-links identified by CXMS and subcellular location of identified cross-linked proteins (XLSX)

Cross-links identified by MitoKit-CXMS, subcellular location of identified cross-linked proteins, and comparison of inter-protein cross-links identified by APEX-CXMS and CXMS of isolated mitochondria reported by Ryl et al. (XLSX)

Cross-links identified by WCL-CXMS (XLSX)

Cross-links identified by APEX-CXMS in the nucleus (XLSX)

Cross-links identified by in vivo CXMS, including the subcellular location of identified cross-linked proteins (XLSX)

AUTHOR INFORMATION

Corresponding Authors

Peng Zou − *Beijing National Laboratory for Molecular Sciences, Key Laboratory of Bioorganic Chemistry and*

https://doi.org/10.1021/acs.analchem.2c02116
Anal. Chem. 2022, 94, 14878−14888

Molecular Engineering of Ministry of Education, Department of Chemical Biology, College of Chemistry and Molecular Engineering, Synthetic and Functional Biomolecules Center, and Peking-Tsinghua Center for Life Sciences, Peking University, Beijing 100871, China; PKU-IDG/McGovern Institute for Brain Research, Peking University, Beijing 100871, China; Chinese Institute for Brain Research (CIBR), Beijing 102206, China; orcid.org/0000-0002-9798-5242; Email: zoupeng@pku.edu.cn

Xiaoguang Lei − *Beijing National Laboratory for Molecular Sciences, Key Laboratory of Bioorganic Chemistry and Molecular Engineering of Ministry of Education, Department of Chemical Biology, College of Chemistry and Molecular Engineering, Synthetic and Functional Biomolecules Center, and Peking-Tsinghua Center for Life Sciences, Peking University, Beijing 100871, China; Institute for Cancer Research, Shenzhen Bay Laboratory, Shenzhen 518107, China;* orcid.org/0000-0002-0380-8035; Email: xglei@pku.edu.cn

Authors

Mengze Sun − *Beijing National Laboratory for Molecular Sciences, Key Laboratory of Bioorganic Chemistry and Molecular Engineering of Ministry of Education, Department of Chemical Biology, College of Chemistry and Molecular Engineering, Synthetic and Functional Biomolecules Center, and Peking-Tsinghua Center for Life Sciences, Peking University, Beijing 100871, China;* orcid.org/0000-0002-8798-4326

Feng Yuan − *Beijing National Laboratory for Molecular Sciences, Key Laboratory of Bioorganic Chemistry and Molecular Engineering of Ministry of Education, Department of Chemical Biology, College of Chemistry and Molecular Engineering, Synthetic and Functional Biomolecules Center, and Peking-Tsinghua Center for Life Sciences, Peking University, Beijing 100871, China*

Yuliang Tang − *Beijing National Laboratory for Molecular Sciences, Key Laboratory of Bioorganic Chemistry and Molecular Engineering of Ministry of Education, Department of Chemical Biology, College of Chemistry and Molecular Engineering, Synthetic and Functional Biomolecules Center, and Peking-Tsinghua Center for Life Sciences, Peking University, Beijing 100871, China*

Complete contact information is available at: https://pubs.acs.org/10.1021/acs.analchem.2c02116

Author Contributions

[1]M.-Z.S. performed the APEX-CXMS and CXMS assay of isolated mitochondria and whole cell lysates, purified proteins for the SPR assay, performed Co-IP, SPR, M2H experiments, analyzed and interpreted the data, and wrote the manuscript; F.Y. provided the mito-APEX2 and 3xNLS-APEX2 HEK293T cells, evaluated the efficiency and specificity of APEX labeling, and revised the manuscript; Y.-L.T. performed the chemical synthesis of the DSS cross-linker, performed MS experiments, and helped with data analysis and interpretation; X.-G.L. guided the study, interpreted the data, and wrote the manuscript; P.Z. guided the study, assisted with data analysis, and revised the manuscript.

Notes

The authors declare no competing financial interest.

■ ACKNOWLEDGMENTS

We thank Prof. Mengqiu Dong (NIBS) for initial mass spectrometry support. We also thank Zhenlin Chen (CAS) for proteomic data analysis script and Fusheng Guo from our lab for valuable experimental materials. Financial support from the National Key Research and Development Program of China (2017YFA0505200 to X.L.; 2018YFA0507600 and 2017YFA0503600 to P.Z.), the National Natural Science Foundation of China Grant (21625201, 21961142010, and 91853202 to X.L.; 32088101 and 21727806 to P.Z.), and the Beijing Outstanding Young Scientist Program (BJJWZYJH01201910001001 to X.L.) is acknowledged. P.Z. was sponsored by the Li Ge-Zhao Ning Life Science Junior Research Fellowship and the Bayer Investigator Award. The measurements of 400 MHz NMR were performed at the Analytical Instrumentation Center of Peking University. The help from PKUAIC Dr. Xiu Zhang is acknowledged.[43]

■ REFERENCES

(1) Braun, P.; Gingras, A. C. *Proteomics* **2012**, *12*, 1478−1498.
(2) Luck, K.; Kim, D. K.; Lambourne, L.; Spirohn, K.; Begg, B. E.; Bian, W.; Brignall, R.; Cafarelli, T.; Campos-Laborie, F. J.; Charloteaux, B.; Choi, D.; Coté, A. G.; Daley, M.; Deimling, S.; Desbuleux, A.; Dricot, A.; Gebbia, M.; Hardy, M. F.; Kishore, N.; Knapp, J. J.; Kovács, I. A.; Lemmens, I.; Mee, M. W.; Mellor, J. C.; Pollis, C.; Pons, C.; Richardson, A. D.; Schlabach, S.; Teeking, B.; Yadav, A.; Babor, M.; Balcha, D.; Basha, O.; Bowman-Colin, C.; Chin, S. F.; Choi, S. G.; Colabella, C.; Coppin, G.; D'Amata, C.; De Ridder, D.; De Rouck, S.; Duran-Frigola, M.; Ennajdaoui, H.; Goebels, F.; Goehring, L.; Gopal, A.; Haddad, G.; Hatchi, E.; Helmy, M.; Jacob, Y.; Kassa, Y.; Landini, S.; Li, R.; van Lieshout, N.; MacWilliams, A.; Markey, D.; Paulson, J. N.; Rangarajan, S.; Rasla, J.; Rayhan, A.; Rolland, T.; San-Miguel, A.; Shen, Y.; Sheykhkarimli, D.; Sheynkman, G. M.; Simonovsky, E.; Taşan, M.; Tejeda, A.; Tropepe, V.; Twizere, J. C.; Wang, Y.; Weatheritt, R. J.; Weile, J.; Xia, Y.; Yang, X.; Yeger-Lotem, E.; Zhong, Q.; Aloy, P.; Bader, G. D.; De Las Rivas, J.; Gaudet, S.; Hao, T.; Rak, J.; Tavernier, J.; Hill, D. E.; Vidal, M.; Roth, F. P.; Calderwood, M. A. *Nature* **2020**, *580*, 402−408.
(3) Park, S. H.; Ko, W.; Lee, H. S.; Shin, I. *J. Am. Chem. Soc.* **2019**, *141*, 4273−4281.
(4) Li, P.; Wang, L.; Di, L. J. *J. Proteome Res.* **2019**, *18*, 2987−2998.
(5) Huttlin, E. L.; Bruckner, R. J.; Paulo, J. A.; Cannon, J. R.; Ting, L.; Baltier, K.; Colby, G.; Gebreab, F.; Gygi, M. P.; Parzen, H.; Szpyt, J.; Tam, S.; Zarraga, G.; Pontano-Vaites, L.; Swarup, S.; White, A. E.; Schweppe, D. K.; Rad, R.; Erickson, B. K.; Obar, R. A.; Guruharsha, K. G.; Li, K.; Artavanis-Tsakonas, S.; Gygi, S. P.; Harper, J. W. *Nature* **2017**, *545*, 505−509.
(6) Yoon, T. Y.; Lee, H. W. *Curr. Opin. Chem. Biol.* **2019**, *53*, 75−81.
(7) Byron, O.; Vestergaard, B. *Curr. Opin. Struct. Biol.* **2015**, *35*, 76−86.
(8) Veres, D. V.; Gyurkó, D. M.; Thaler, B.; Szalay, K. Z.; Fazekas, D.; Korcsmáros, T.; Csermely, P. *Nucleic Acids Res.* **2015**, *43*, D485−D493.
(9) Song, J.; Herrmann, J. M.; Becker, T. *Nat. Rev. Mol. Cell Biol.* **2021**, *22*, 54−70.
(10) Schweppe, D. K.; Chavez, J. D.; Lee, C. F.; Caudal, A.; Kruse, S. E.; Stuppard, R.; Marcinek, D. J.; Shadel, G. S.; Tian, R.; Bruce, J. E. *Proc. Natl. Acad. Sci. U.S.A.* **2017**, *114*, 1732−1737.
(11) Liu, F.; Lössl, P.; Rabbitts, B. M.; Balaban, R. S.; Heck, A. J. R. *Mol. Cell. Proteomics* **2018**, *17*, 216−232.
(12) Ryl, P. S. J.; Bohlke-Schneider, M.; Lenz, S.; Fischer, L.; Budzinski, L.; Stuiver, M.; Mendes, M. M. L.; Sinn, L.; O'Reilly, F. J.; Rappsilber, J. *J. Proteome Res.* **2020**, *19*, 327−336.
(13) Linden, A.; Deckers, M.; Parfentev, I.; Pflanz, R.; Homberg, B.; Neumann, P.; Ficner, R.; Rehling, P.; Urlaub, H. *Mol. Cell. Proteomics* **2020**, *19*, 1161−1178.

(14) Rhee, H. W.; Zou, P.; Udeshi, N. D.; Martell, J. D.; Mootha, V. K.; Carr, S. A.; Ting, A. Y. *Science* **2013**, *339*, 1328−1331.
(15) Hung, V.; Zou, P.; Rhee, H. W.; Udeshi, N. D.; Cracan, V.; Svinkina, T.; Carr, S. A.; Mootha, V. K.; Ting, A. Y. *Mol. Cell* **2014**, *55*, 332−341.
(16) Lam, S. S.; Martell, J. D.; Kamer, K. J.; Deerinck, T. J.; Ellisman, M. H.; Mootha, V. K.; Ting, A. Y. *Nat. Methods* **2015**, *12*, 51−54.
(17) Choi-Rhee, E.; Schulman, H.; Cronan, J. E. *Protein Sci.* **2004**, *13*, 3043−50.
(18) Roux, K. J.; Kim, D. I.; Raida, M.; Burke, B. *J. Cell Biol.* **2012**, *196*, 801−810.
(19) Branon, T. C.; Bosch, J. A.; Sanchez, A. D.; Udeshi, N. D.; Svinkina, T.; Carr, S. A.; Feldman, J. L.; Perrimon, N.; Ting, A. Y. *Nat. Biotechnol.* **2018**, *36*, 880−887.
(20) Liu, F.; Heck, A. J. *Curr. Opin. Struct. Biol.* **2015**, *35*, 100−108.
(21) Leitner, A.; Faini, M.; Stengel, F.; Aebersold, R. *Trends Biochem. Sci.* **2016**, *41*, 20−32.
(22) Tan, D.; Li, Q.; Zhang, M.; Liu, C.; Ma, C.; Zhang, P.; Ding, Y.; Fan, S.; Tao, L.; Yang, B.; Li, X.; Ma, S.; Liu, J.; Feng, B.; Liu, X.; Wang, H.; He, S.; Gao, N.; Ye, K.; Dong, M.; Lei, X. *Elife* **2016**, *5*, No. e12509.
(23) Sinz, A. *Angew. Chem., Int. Ed. Engl.* **2018**, *57*, 6390−6396.
(24) O'Reilly, F. J.; Rappsilber, J. *Nat. Struct. Mol. Biol.* **2018**, *25*, 1000−1008.
(25) Yu, C.; Huang, L. *Anal. Chem.* **2018**, *90*, 144−165.
(26) Chavez, J. D.; Bruce, J. E. *Curr. Opin. Chem. Biol.* **2019**, *48*, 8−18.
(27) Lee, S. Y.; Kang, M. G.; Shin, S.; Kwak, C.; Kwon, T.; Seo, J. K.; Kim, J. S.; Rhee, H. W. *J. Am. Chem. Soc.* **2017**, *139*, 3651−3662.
(28) Lee, S. Y.; Seo, J. K.; Rhee, H. W. *Methods Mol. Biol.* **2019**, *2008*, 97−105.
(29) Lee, S. Y.; Lee, H.; Lee, H. K.; Lee, S. W.; Ha, S. C.; Kwon, T.; Seo, J. K.; Lee, C.; Rhee, H. W. *ACS Cent. Sci.* **2016**, *2*, 506−516.
(30) Park, J.; Lee, S. Y.; Jeong, H.; Kang, M. G.; Van Haute, L.; Minczuk, M.; Seo, J. K.; Jun, Y.; Myung, K.; Rhee, H. W.; Lee, C. *Nucleic Acids Res.* **2019**, *47*, 7078−7093.
(31) Yoo, C. M.; Rhee, H. W. *Biochemistry* **2020**, *59*, 250−259.
(32) Liu, C. H.; Chien, M. J.; Chang, Y. C.; Cheng, Y. H.; Li, F. A.; Mou, K. Y. *J. Proteome Res.* **2020**, *19*, 1109−1118.
(33) Jones, A. X.; Cao, Y.; Tang, Y.; Wang, J.; Ding, Y.; Tan, H.; Chen, Z.; Fang, R.; Yin, J.; Chen, R.; Zhu, X.; She, Y.; Huang, N.; Shao, F.; Ye, K.; Sun, R.; He, S.; Lei, X.; Dong, M. *Nat. Commun.* **2019**, *10*, 3911−3921.
(34) Han, S.; Udeshi, N. D.; Deerinck, T. J.; Svinkina, T.; Ellisman, M. H.; Carr, S. A.; Ting, A. Y. *Cell Chem. Biol.* **2017**, *24*, 404−414.
(35) Li, R.; Zou, Z.; Wang, W.; Zou, P. *Cell Chem. Biol.* **2022**, *29*, 1−14.
(36) Leitner, A.; Walzthoeni, T.; Aebersold, R. *Nat. Protoc.* **2014**, *9*, 120−137.
(37) Chen, Z.; Meng, J.; Cao, Y.; Yin, J.; Fang, R.; Fan, S.; Liu, C.; Zeng, W.; Ding, Y.; Tan, D.; Wu, L.; Zhou, W.; Chi, H.; Sun, R.; Dong, M.; He, S. *Nat. Commun.* **2019**, *10*, 3404−3415.
(38) Yang, J.; Li, B.; He, Q. *Cell Death Dis* **2018**, *9*, 580−589.
(39) Gottschling, D. E.; Nyström, T. *Cell* **2017**, *169*, 24−34.
(40) Kaake, R. M.; Wang, X.; Burke, A.; Yu, C.; Kandur, W.; Yang, Y.; Novtisky, E. J.; Second, T.; Duan, J.; Kao, A.; Guan, S.; Vellucci, D.; Rychnovsky, S. D.; Huang, L. *Mol. Cell. Proteomics* **2014**, *13*, 3533−3543.
(41) Wheat, A.; Yu, C.; Wang, X.; Burke, A. M.; Chemmama, I. E.; Kaake, R. M.; Baker, P.; Rychnovsky, S. D.; Yang, J.; Huang, L. *Proc. Natl. Acad. Sci. U.S.A.* **2021**, *118*, 1−12.
(42) Jiang, P.; Wang, C.; Diehl, A.; Viner, R.; Etienne, C.; Nandhikonda, P.; Foster, L.; Bomgarden, R. D.; Liu, F. *Angew. Chem., Int. Ed. Engl.* **2021**, No. e202113937.
(43) Fields, S.; Song, O. *Nature* **1989**, *340*, 245−246.

https://doi.org/10.1021/acs.analchem.2c02116
Anal. Chem. 2022, 94, 14878−14888